INTERNATIONAL JOURNAL OF OPTIMIZATION IN CIVIL ENGINEERING
Int. J. Optim. Civil Eng., 2026; 16(2):301-324

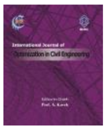

UNCERTAINTY QUANTIFICATION IN APPROXIMATING DYNAMIC RESPONSES OF STRUCTURES USING REDUCED ORDER MODELS

S. Maleki, M. Ilchi Ghazaan[*,†], and A. Ghafouri
School of Civil Engineering, Iran University of Science and Technology, P.O. Box 16846-13114, Iran

[DOI: 10.22068/ijoce.2026.16.2.679]

ABSTRACT

Reduced order models (ROMs) are widely used to approximate the dynamic response of large-scale structural systems while substantially reducing computational cost. Inherent uncertainties necessitate the assessment of ROMs within an uncertainty quantification (UQ) framework. Although the deterministic accuracy of reduction techniques has been extensively investigated, their capability for UQ remains insufficiently understood. This study presents a systematic UQ-based assessment of four condensation techniques: Guyan reduction, dynamic condensation, Improved Reduced System (IRS), and the System Equivalent Reduction Expansion Process (SEREP). A shear frame and a plane truss are used to evaluate the combined influence of the reduction technique, master degree of freedom (DOF) selection, and structural dynamic complexity on ROM predictive capability. Polynomial Chaos Expansion (PCE) is employed for UQ, and variance-based Sobol' indices are adopted for global sensitivity analysis (GSA). SEREP consistently provides the closest approximation to the full order model, whereas IRS also maintains high accuracy over most vibration modes. The accuracy of the Guyan and dynamic condensation methods decreases as higher-order dynamics become increasingly important.

Keywords: Reduced order models; Uncertainty quantification; Polynomial Chaos Expansion; Global sensitivity analysis; Structural dynamics.

Received: 26 March 2026; Accepted: 28 May 2026

---

[*] Corresponding author: School of Civil Engineering, Iran University of Science and Technology, P.O. Box 16846-13114, Iran
[†]E-mail address: ilchi@iust.ac.ir (M. Ilchi Ghazaan)

[DOI: 10.22068/ijoce.2026.16.2.679]

1. INTRODUCTION

The dynamic behaviour of structures is strongly influenced by their vibrational characteristics, which are primarily determined by the distribution of mass and stiffness. Among these parameters, natural frequencies are of particular importance. Resonance occurs when the excitation frequency approaches a natural frequency, leading to excessive structural vibrations that may compromise structural performance and safety [1-3]. This issue becomes increasingly significant for large-scale structural systems, where dynamic analyses often involve substantial computational demands.

Model order reduction (MOR) techniques have emerged as an efficient framework for reducing the computational cost of structural dynamic analysis. By decreasing the number of degrees of freedom (DOFs), these methods improve computational efficiency while retaining the essential dynamic characteristics of the original structure [4-6].

Numerous studies have investigated condensation-based reduced order models (ROMs) in structural dynamics, demonstrating that the performance of these techniques depends on both the adopted reduction strategy and the characteristics of the underlying structural system [4, 7, 8]. Various condensation techniques, including Guyan reduction, dynamic condensation, Improved Reduced System (IRS), and the System Equivalent Reduction Expansion Process (SEREP), have been developed to offer varying levels of computational efficiency while maintaining predictive accuracy. Owing to their distinct theoretical assumptions and numerical formulations, these methods exhibit varying levels of fidelity across diverse structural applications, making the selection of an appropriate condensation strategy a critical factor in obtaining reliable reduced order predictions.

Uncertainties in structures arise from multiple interacting sources that can affect the reliability of numerical predictions [9]. These uncertainties originate not only from inherent variability in material properties, geometric imperfections, boundary conditions, and external loads, but also from limitations in measured data, including noise, missing information, and experimental inaccuracies [10, 11]. Moreover, modelling assumptions and numerical simplifications can further contribute to deviations in predicted structural responses.

Within this context, reduced order representations inherently involve approximation errors because reducing the system dimension may affect the dynamic response of the full order model (FOM). The extent to which different condensation techniques can reliably propagate input uncertainties while maintaining the computational advantages of model reduction remains an important research question.

To improve the reliability of predictions under such uncertain conditions, uncertainty quantification (UQ) provides a rigorous framework for characterizing uncertainties and evaluating their effects on structural responses. By enabling the systematic assessment of uncertainty propagation within computational models, UQ facilitates more reliable predictions, supports model validation, and enhances confidence in numerical simulations [12-14]. Its integration into computational mechanics has become increasingly important for addressing uncertainty-driven challenges and supporting robust engineering decisions [15].

Monte Carlo simulation (MCS) is among the most established techniques for UQ, enabling probabilistic assessment of structural responses through repeated random sampling [16]. Despite its reliability and broad applicability, MCS requires a large number of samples to achieve statistical convergence, which may lead to significant resource requirements, particularly for high-fidelity finite element analyses [17].

To overcome the high cost associated with repeated evaluations in MCS, surrogate modelling techniques have been developed as efficient alternatives for approximating computationally demanding models. These methods use data from numerical simulations or experiments to approximate high-fidelity model responses, enabling rapid predictions while maintaining acceptable accuracy [18-20]. Among various surrogate approaches, Polynomial Chaos Expansion (PCE) has attracted considerable attention in UQ due to its mathematical foundation and ability to represent stochastic responses using orthogonal polynomial expansions. The coefficients of the resulting expansion provide quantitative insight into the contribution of input uncertainties to the variability of the system response [21-24].

The applicability of PCE has been validated in a wide range of structural engineering problems, from simplified benchmark examples to full-scale structural systems. Previous studies have reported strong agreement between PCE predictions and MCS results, while requiring substantially fewer model evaluations, demonstrating its capability for uncertainty quantification and sensitivity analysis of structural responses [25, 26].

Sensitivity analysis (SA) complements UQ by examining how uncertainties associated with model inputs affect variations in predicted responses [27]. To account for interactions among multiple uncertain parameters, global sensitivity analysis (GSA) provides a comprehensive assessment of input–output relationships by identifying the relative influence of uncertain parameters on the variability of structural responses [28]. This information is particularly valuable in structural engineering, where recognizing the most influential sources of uncertainty can support informed modelling decisions and improve the reliability of computational analyses.

The Sobol method is frequently employed in GSA because of its variance-based decomposition of model outputs into effects associated with individual uncertain parameters and their combined influence. This formulation enables quantitative evaluation of parameter importance and provides insight into the relative role of uncertain inputs in governing the variability of structural responses. Previous investigations have applied the Sobol method to various engineering problems, verifying its suitability for uncertainty analysis in systems involving multiple uncertain variables [29-31].

The present study investigates the performance of four condensation methods, namely Guyan reduction, dynamic condensation, IRS, and SEREP, for approximating structural responses in the presence of uncertainties. Unlike deterministic assessments, this work provides a systematic evaluation of these techniques under uncertain conditions and examines their ability to deliver reliable frequency predictions for structures with different dynamic behavior.

The uncertainties considered in this study originate from variability in material properties and geometric parameters. Their effects on natural frequency predictions are evaluated through UQ and GSA using two benchmark systems exhibiting different dynamic characteristics: a shear frame with a relatively narrow frequency range (approximately $2-40\ Hz$) and a plane truss spanning a much broader range (approximately $20-2000\ Hz$).

The main contributions of this study include three key aspects. First, it evaluates how the selection of retained DOFs influences the accuracy of natural frequency prediction. Second, it examines how input uncertainties affect structural responses predicted by ROMs. Finally, it

[DOI: 10.22068/ijoce.2026.16.2.679]

applies GSA to compare ROMs and FOMs, providing insight into the relative advantages and limitations of different reduction strategies.

The remainder of this paper is organized as follows. Section 2 presents the methodology, including the condensation techniques, PCE-based UQ framework, and Sobol method for GSA. Section 3 describes the numerical models and the adopted DOF reduction procedure. Section 4 discusses the results, focusing on the comparative performance of the condensation techniques, uncertainty effects, and sensitivity assessment. Finally, Section 5 summarizes the main conclusions of this study.

2. METHODOLOGY

This section outlines the methodology for assessing the accuracy of the considered MOR techniques in approximating structural responses under uncertain conditions. It involves four condensation methods, namely Guyan reduction, dynamic condensation, IRS, and SEREP, together with PCE-based UQ and the Sobol method for GSA.

2.1 Condensation methods

Condensation techniques reduce the number of DOFs by retaining a subset of the original coordinates while eliminating the remaining ones. Accordingly, the DOFs are partitioned into master (m) and slave (s) subsets. Based on this partitioning, the governing equation of motion for an n-DOF system can be written as follows [7]:

$$M\ddot{u} + C\dot{u} + Ku = f \tag{1}$$

Here, $M,\ C,\ K \in \mathbb{R}^{n\times n}$ denotes the mass, damping, and stiffness matrices, respectively, while $f = f(t) \in \mathbb{R}^{n\times 1}$ is the load vector, and $u = u(t) \in \mathbb{R}^{n\times 1}$ represents the state vector of interest in condensation methods, m master DOFs are selected to remain in the system during the reduction process. The state vector is then approximated as $u = Tu_R$, where $T\epsilon\mathbb{R}^{n\times m}$ is the transformation matrix, and $u_R \in \mathbb{R}^{m\times 1}$ represents the reduced state vector. This transformation leads to the following equations:

$$M_R\ddot{u}_R + C_R\dot{u}_R + K_R u_R = f_R \tag{2}$$

$$M_R = T^T MT,\quad C_R = T^T CT,\quad K_R = T^T KT,\quad f_R = T^T f \tag{3}$$

Where $M_R,\ C_R,\ K_R \in R^{m\times m}$ are the reduced mass, damping, and stiffness matrices, respectively, and $f_R \in \mathbb{R}^{m\times 1}$ denotes the reduced load vector. The distinction among the condensation techniques lies in the formulation of the transformation matrix T, which is described for each method in the following subsections.

2.1.1 Guyan reduction

The Guyan reduction, also known as static condensation, is based on the assumption that the inertia effects associated with the eliminated DOFs are negligible [32]. The eliminated

[DOI: 10.22068/ijoce.2026.16.2.679]

coordinates can therefore be expressed solely in terms of the retained DOFs, resulting in a reduced order representation of the full model. The following formulation is based on [7].
Partitioning the state vector into master and slave components allows the matrices in Eq. (1) to be expressed as follows:

$$\begin{bmatrix} M_{mm} & M_{ms} \\ M_{sm} & M_{ss} \end{bmatrix} \begin{bmatrix} \ddot{u}_m \\ \ddot{u}_s \end{bmatrix} + \begin{bmatrix} K_{mm} & K_{ms} \\ K_{sm} & K_{ss} \end{bmatrix} \begin{bmatrix} u_m \\ u_s \end{bmatrix} = \begin{bmatrix} f_m \\ f_s \end{bmatrix} \tag{4}$$

It is assumed that no external forces are applied to the slave DOFs, resulting in the following equation:

$$u_s = -K_{ss}{}^{-1}(M_{sm}\ddot{u}_m + M_{ss}\ddot{u}_s + K_{sm}u_m) \tag{5}$$

Neglecting the inertia terms yields the following transformation matrix for the Guyan reduction:

$$\begin{bmatrix} u_m \\ u_s \end{bmatrix} = \begin{bmatrix} I \\ -K_{ss}{}^{-1}K_{sm} \end{bmatrix} u_m = T_{Guyan}u_m \tag{6}$$

2.1.2 Dynamic condensation

Unlike the Guyan reduction, dynamic condensation accounts for the inertia effects associated with the eliminated DOFs by introducing a frequency-dependent transformation matrix [33, 34]. The mathematical formulation is summarized below [35].
The partitioned equation of motion for the system, excluding external forces, is expressed as follows:

$$\begin{bmatrix} M_{mm} & M_{ms} \\ M_{sm} & M_{ss} \end{bmatrix} \begin{bmatrix} \ddot{u}_m \\ \ddot{u}_s \end{bmatrix} + \begin{bmatrix} K_{mm} & K_{ms} \\ K_{sm} & K_{ss} \end{bmatrix} \begin{bmatrix} u_m \\ u_s \end{bmatrix} = \begin{bmatrix} 0 \\ 0 \end{bmatrix} \tag{7}$$

It is assumed that the master and slave state vectors are defined as follows:

$$u_m = \overline{u}_m \cos \omega t \tag{8}$$

$$u_s = \overline{u}_s \cos \omega t \tag{9}$$

These values are substituted into Eq. (7), resulting in the following equation:

$$\begin{bmatrix} K_{mm} - \omega^2 M_{mm} & K_{ms} - \omega^2 M_{ms} \\ K_{sm} - \omega^2 M_{sm} & K_{ss} - \omega^2 M_{ss} \end{bmatrix} \begin{bmatrix} \overline{u}_m \\ \overline{u}_s \end{bmatrix} = \begin{bmatrix} 0 \\ 0 \end{bmatrix} \tag{10}$$

Substituting the equations from the Guyan reduction into Eq. (10) yields the transformation matrix for the dynamic condensation method, expressed as follows:

[DOI: 10.22068/ijoce.2026.16.2.679]

$$T_{\text{Dynamic}} = \begin{bmatrix} I_{m\times m} \\ [K_{ss} - \omega^2 M_{ss}]^{-1}[K_{sm} - \omega^2 M_{sm}] \end{bmatrix}_{n\times m} \tag{11}$$

2.1.3 Improved reduced system (IRS)

The IRS method extends the Guyan reduction by introducing an inertia correction to improve the accuracy of the reduced model. Unlike the Guyan reduction, which neglects the inertia contribution of the eliminated DOFs, the IRS method incorporates these effects as pseudo-static forces. The theoretical formulation is presented below [7, 36].
In the Guyan reduction, the accelerations of the master and slave DOFs are computed as follows:

$$\ddot{u}_m = M_{Guyan}^{-1} K_{Guyan} u_m \tag{12}$$

$$\ddot{u}_s = -K_{ss}{}^{-1} K_{sm} \ddot{u}_m = K_{ss}{}^{-1} K_{sm} M_{Guyan}^{-1} K_{Guyan} u_m \tag{13}$$

Substituting Eqs. (12) and (13) into Eq. (5) results in the following equation:

$$u_s = K_{ss}{}^{-1}(M_{sm} M_{Guyan}^{-1} K_{Guyan} - M_{ss} K_{ss}{}^{-1} K_{sm} M_{Guyan}^{-1} K_{Guyan} - K_{sm}) u_m \tag{14}$$

For the IRS method, the transformation matrix is expressed as:

$$T_{IRS} = T_{Guyan} + SMT_{Guyan} M_{Guyan}^{-1} K_{Guyan} \tag{15}$$

$$S = \begin{bmatrix} 0 & 0 \\ 0 & K_{ss}{}^{-1} \end{bmatrix} \tag{16}$$

2.1.4 System equivalent expansion reduction process (SEREP)

The SEREP method derives the transformation matrix directly from the modal information of the FOM. The transformation is established using the eigenvectors associated with the retained DOFs, providing a reduced order representation of the original system [37]. The formulation of the SEREP method is defined below [4].

The state vector u is related to the modal coordinates q through the modal matrix ψ, as given by:

$$u = \psi q \tag{17}$$

The state vector and the modal matrix are partitioned into master and slave components, leading to:

$$u = \begin{bmatrix} u_m \\ u_s \end{bmatrix} = \begin{bmatrix} \psi_m \\ \psi_s \end{bmatrix} q \tag{18}$$

Applying the pseudoinverse of ψ_m yields the transformation matrix for the SEREP method:

[DOI: 10.22068/ijoce.2026.16.2.679]

$$\begin{bmatrix} u_m \\ u_s \end{bmatrix} = \begin{bmatrix} \psi_m \\ \psi_s \end{bmatrix} \psi_m^+ u_m = T_{SEREP} u_m \tag{19}$$

where $\psi_m^+ = (\psi_m^T \psi_m)^{-1} \psi_m^T$ denotes the pseudoinverse of ψ_m.

2.1.5 Evaluation metric

The accuracy of the ROMs is evaluated by comparing the natural frequencies predicted by each condensation method with those of the corresponding FOM. For this purpose, the normalised relative frequency difference (NRFD) is employed as the performance metric, providing a quantitative measure of the discrepancy between the natural frequencies predicted by the FOM and ROM. Lower NRFD values indicate closer agreement with the reference solution and, consequently, higher prediction accuracy. The NRFD can be expressed as [38]:

$$NRFD(i) = \left| 1 - \frac{f_{full}(i)}{f_{red}(i)} \right| \times 100\% \tag{20}$$

Here, $f_{full}(i)$ represents the frequency of the full model in the i-th mode, and $f_{red}(i)$ denotes the frequency of the reduced model in the i-th mode.

2.2 Uncertainty quantification and global sensitivity analysis framework

This study integrates PCE and Sobol-based GSA for uncertainty analysis of the ROMs. PCE is employed to efficiently propagate input uncertainties and provide a surrogate model for the predicted natural frequencies, whereas Sobol's method quantifies the contribution of each uncertain parameter to the output variance. Together, these methods enable a comprehensive assessment of uncertainty propagation and parameter sensitivity in the reduced models.

2.2.1 Polynomial chaos expansion (PCE)

PCE approximates a quantity of interest (QoI), denoted as Y, which depends on uncertain input variables, X, through a series of orthogonal polynomials. This technique is particularly valuable for reducing computational effort in UQ while preserving statistical accuracy. By utilizing polynomial expansions to represent the system's response, PCE provides a robust framework for analyzing complex models. The mathematical formulation of PCE is given as follows [19]:

The response Y, assumed to have finite variance (i.e. $\mathbb{E}[Y^2] \leq +\infty$), is expressed as a series expansion of multivariate polynomial basis functions $\psi_\alpha(X)$, as follows:

$$Y = \sum_{\alpha \in \mathbb{N}^M} y_\alpha \, \psi_\alpha(X) \tag{21}$$

[DOI: 10.22068/ijoce.2026.16.2.679]

Here, M represents the number of input variables, y_α are the coefficients of the expansion, and $\psi_\alpha(X) = \prod_{i=1}^{M} \pi_{\alpha_i}^{(i)}(x_i)$ is the multivariate basis function defined as the product of univariate orthogonal polynomials $\pi_{\alpha_i}^{(i)}(x_i)$.

The set $\{\pi_k^{(i)},\ k \in \mathbb{N}\}$ denotes a family of univariate orthonormal polynomials with respect to the marginal probability density function f_{X_i}. The polynomial basis functions $\pi_{\alpha_i}^{(i)}(x_i)$ satisfy the following orthogonality condition:

$$\langle \pi_j^{(i)}, \pi_k^{(i)} \rangle = \int \pi_j^{(i)}(u)\pi_k^{(i)}(u) f_{X_i}(u) du = \delta_{jk} \tag{22}$$

where δ_{jk} is the Kronecker delta. Multivariate orthogonality then follows as $\mathbb{E}[\psi_\alpha(X)\psi_\beta(X)] = \delta_{\alpha\beta}$.

To make computations feasible, a truncation scheme is applied to limit the number of polynomial basis functions in the expansion. The standard truncation approach involves selecting only those polynomials whose total degree p_t, which is the sum of the multi-indices α_i across all dimensions ($p_t = \sum_{i=1}^{M} \alpha_i$), is less than or equal to a predefined maximum degree p. This leads to the truncated representation of the model response Y, expressed as:

$$Y = \mathcal{M}(X) \approx \sum_{\alpha \in \mathcal{A}} y_\alpha \psi_\alpha(X) + \varepsilon \tag{23}$$

where the truncation set $\mathcal{A} = \{\alpha: \sum_{i=1}^{M} \alpha_i \le p\}$ is defined as the collection of all multi-indices α whose total degree does not exceed p.

The cardinality P of the truncation set, which represents the total number of retained polynomial terms, is given by $P = \binom{M+p}{p}$. This equation accounts for all possible combinations of polynomial degrees up to p across the M input dimensions. Once this truncation set is defined, various techniques can be used to estimate the coefficients y_α. Among them, least-squares minimization is a widely used and effective approach.

The coefficients y_α are computed by minimizing the mean square error (MSE) between the true model response $\mathcal{M}(X)$ and its PCE approximation. This minimization is mathematically expressed as:

$$\hat{y} = \arg\min_{y_\alpha} \mathbb{E}\left[\left(\mathcal{M}(X) - \sum_{\alpha \in \mathcal{A}} y_\alpha \psi_\alpha(X)\right)^2\right] \tag{24}$$

For practical purposes, the expectation in the minimization problem is approximated using n experimental design samples, $\{\mathcal{X}^{(i)},\ \mathcal{M}(\mathcal{X}^{(i)})\}_{i=1}^{n}$. The discrete approximation of the MSE is then expresed as:

[DOI: 10.22068/ijoce.2026.16.2.679]

$$\hat{y} = \arg\min_{y_\alpha} \frac{1}{n}\sum_{i=1}^{n}\left(\mathcal{M}\big(\mathcal{X}^{(i)}\big) - \sum_{\alpha\in\mathcal{A}} y_\alpha \psi_\alpha\big(\mathcal{X}^{(i)}\big)\right)^2 \tag{25}$$

The computation can be efficiently expressed in matrix form. In this formulation, the experimental matrix A is defined such that each entry is given by:

$$A_{ij} = \psi_j\big(\mathcal{X}^{(i)}\big), \quad where \quad i \in \{1,\ 2, \dots ,\ n\}, \quad j \in \{0,\ 1, \dots ,\ P-1\} \tag{26}$$

The vector $\mathrm{M} = \left\{\mathcal{M}\big(\mathcal{X}^{(1)}\big), \dots, \mathcal{M}\big(\mathcal{X}^{(n)}\big)\right\}^T$ contains the model evaluations at all design points. The least-squares solution for the coefficient vector $\hat{y}$ is then determined as:

$$\hat{y} = (A^T A)^{-1} A^T M \tag{27}$$

To evaluate the accuracy of the PCE approximation, a built-in error estimate can be derived using leave-one-out (LOO) cross-validation. The generalization error E_{gen}, which measures the expected squared difference between the true model $\mathcal{M}(X)$ and its PCE approximation $\mathcal{M}^{PCE}(X)$, is expressed as:

$$E_{gen} = \mathbb{E}\left[\big(\mathcal{M}(X) - \mathcal{M}^{PCE}(X)\big)^2\right] \tag{28}$$

In practice, this error is approximated using the LOO approach, which is defined as:

$$E_{\mathrm{LOO}} = \frac{1}{n}\sum_{i=1}^{n} \frac{\left(\mathcal{M}\big(\mathcal{X}^{(i)}\big) - \mathcal{M}^{\mathrm{PCE}}\big(\mathcal{X}^{(i)}\big)\right)^2}{(1-h_i)^2} \tag{29}$$

where h_i represents the i-th diagonal entry of the projection matrix $A(A^T A)^{-1} A^T$.
From the orthogonality of the basis, the statistical moments of Y can be directly derived. The mean and variance are:

$$\hat{\mu}_Y = \hat{y}_0 \qquad \hat{\sigma}_Y^2 = \sum_{\alpha\in\mathcal{A}\setminus 0} \hat{y}_\alpha^2 \tag{30}$$

Additionally, the truncated expansion $\widetilde{\mathcal{M}} = \sum_{\alpha\in\mathcal{A}} \hat{y}_\alpha \psi_\alpha(x)$ is employed as a surrogate model for efficient sampling or UQ.

2.2.2 Sobol sensitivity analysis

Sobol-based GSA quantifies the contributions of uncertain input parameters and their interactions to the variance of the model response through a variance-based decomposition [39, 40]. The resulting sensitivity indices distinguish the individual and interaction effects of

[DOI: 10.22068/ijoce.2026.16.2.679]

the input parameters, thereby identifying the dominant sources of output uncertainty [41, 42]. The Sobol method is mathematically formulated as described by the following equations [43].

The stochastic model is presented as $Y = \mathcal{M}(X)$, where X is a random input vector consisting of independent parameters, and Y represents the QoI. The Sobol decomposition of Y can be expressed as follows:

$$Y = \mathcal{M}_0 + \sum_{i=1}^{n} \mathcal{M}_i\,(X_i) + \sum_{1 \le i < j \le n} \mathcal{M}_{ij}\big(X_i, X_j\big) + \cdots + \mathcal{M}_{1\ldots m}(X_i, \ldots, X_n) \tag{31}$$

With

$$\begin{gathered} \mathcal{M}_0 = \mathbb{E}[Y] \\ \mathcal{M}_i(X_i) = \mathbb{E}[Y|X_i] - \mathcal{M}_0 \\ \mathcal{M}_{ij}\big(X_i, X_j\big) = \mathbb{E}\big[Y\big|X_i, X_j\big] - \mathcal{M}_0 - \mathcal{M}_i - \mathcal{M}_j \end{gathered} \tag{32}$$

$\mathcal{M}_0$ is the mean of the response, and the subsequent terms capture the effects of individual inputs, their pairwise interactions, and higher-order combinations. Each term is recursively defined as a conditional expectation, forming an orthogonal decomposition. This provides a structured representation of how input uncertainties contribute to the model's response variability, leading to the following expression for the total variance:

$$Var(Y) = \sum_{u} Var\big(\mathcal{M}_u(X_u)\big), \quad \emptyset \neq u \subset \{1, \ldots, n\} \tag{33}$$

The conditional variance $Var\big(\mathcal{M}_u(X_u)\big)$ quantifies the contribution of the subset of input variables X_u to the total output variance, where X_u denotes the variables indexed by the subset u. The Sobol' index associated with the subset u is then defined as the ratio of this contribution to the total model variance:

$$S_u = \frac{Var\big(\mathcal{M}_u(X_u)\big)}{Var(Y)} \tag{34}$$

From this equation, it follows that:

$$\sum_{u} S_u = \sum_{i=1}^{n} S_i + \sum_{1 \le i < j \le n} S_{ij} + \cdots + S_{1\ldots m} = 1 \tag{35}$$

The first-order and second-order Sobol' indices are respectively defined as:

$$S_i = \frac{Var(\mathcal{M}_i(X_i))}{Var(Y)}\,, \quad i = 1, \ldots, n \tag{36}$$

[DOI: 10.22068/ijoce.2026.16.2.679]

$$S_{ij} = \frac{Var\left(\mathcal{M}_{ij}(X_{ij})\right)}{Var(Y)}, \quad 1 \leq i < j \leq n \tag{37}$$

where S_i quantifies the individual contribution of the input variable X_i to the total output variance, whereas S_{ij} represents the contribution arising from the interaction between the input variables X_i and X_j. Higher-order Sobol' indices are formulated in an analogous manner and quantify the contributions associated with interactions among three or more input variables. The total Sobol' indices are used to measure the full contribution of the i-th random variable X_i to the total variance, considering both its individual effect and its interactions with other variables. These indices are defined as follows:

$$S_{Ti} = \sum_{u \subset \{1,\ldots,n\},\ i \in u} S_u, \quad i = 1, \ldots, n \tag{38}$$

3. NUMERICAL MODELS

This section describes the numerical models, uncertain input parameters, and DOF reduction strategies used for assessing the performance of the ROMs. These components establish the basis for evaluating the accuracy of the condensation techniques in predicting natural frequencies under uncertain conditions.

3.1 Description of numerical models

Two structural models, namely a shear frame and a plane truss, are adopted to assess the performance of the four reduction techniques studied in this work [8].

The shear frame, shown in Figure 1, is a 16-story structure with three spans of 7 m each and a floor height of 3 m. For dynamic analysis, only the horizontal translational displacement at each floor is considered, resulting in a model with 16 DOFs. This simplified representation enables the evaluation of the investigated ROM techniques for a low-frequency structural system.

The plane truss, shown in Figure 2, consists of 14 nodes and 25 elements. Each node has two translational DOFs corresponding to the horizontal and vertical directions, resulting in a total of 28 DOFs. Given its broader frequency range, this model is employed to examine the performance of the investigated ROM techniques in reproducing the dynamic behavior of the FOM.

3.2 Uncertain input parameters

In the shear frame model, the uncertain input parameters are the moments of inertia of the columns $(I_1 - I_8)$. These parameters are assumed to follow the probability distributions reported in [44]. The corresponding probability distributions and statistical properties are listed in Table 1.

In the plane truss model, the uncertain input parameters are Young's modulus (E), mass density (ρ), the cross-sectional areas of the horizontal (A_1) and vertical/diagonal (A_2)

[DOI: 10.22068/ijoce.2026.16.2.679]

members, and the lengths of the horizontal (L_1) and vertical (L_2) members. The probability distributions assigned to these parameters are selected based on previous studies [25, 45, 46]. The corresponding statistical properties are summarized in Table 2.

3.3 Master degree of freedom selection strategies

To investigate the effect of master DOF selection on the performance of the ROMs, three distinct selection strategies are considered. Each strategy defines a different set of retained master DOFs, providing alternative condensation configurations for representing the dynamic behavior of the FOM. This enables a systematic comparison of the reduction methods while examining how the selection of master DOFs influences the accuracy of the predicted dynamic responses under uncertainty. The retained master DOFs for the shear frame and plane truss are listed in Tables 3 and 4, respectively, following the master DOF configurations proposed in [8].

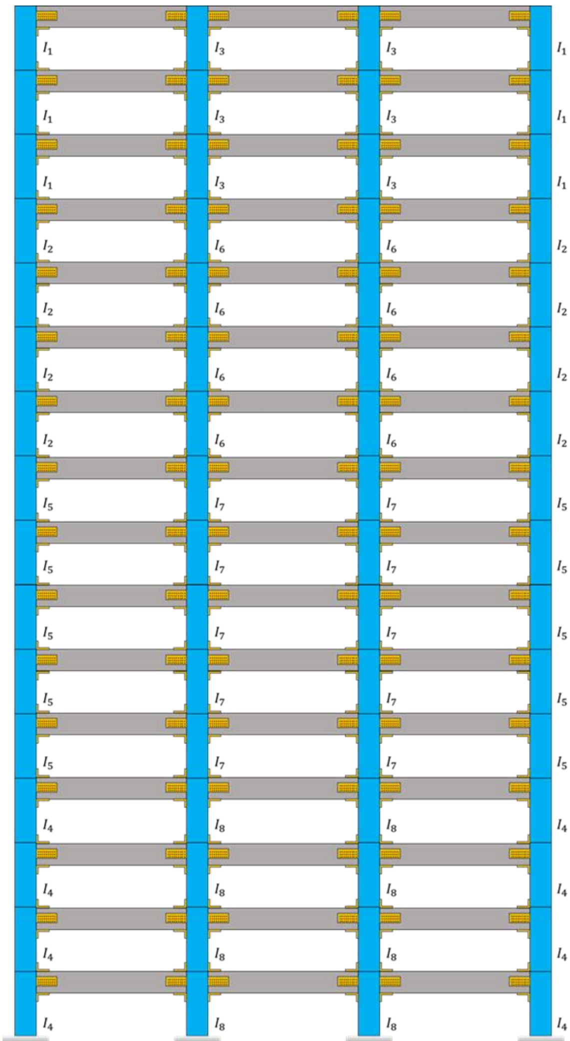

Figure 1: Configuration of the shear frame

[DOI: 10.22068/ijoce.2026.16.2.679]

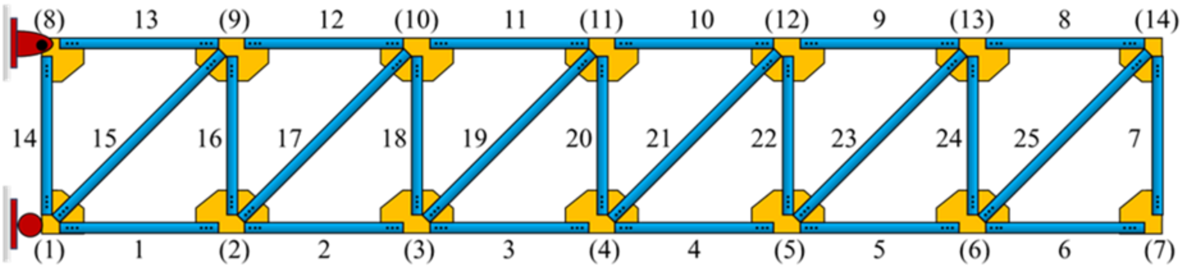

Figure 2: Configuration of the plane truss

Table 1: Description of the input uncertainties and their statistical properties for the shear frame

Parameter	Distribution	Unit	Mean	Std. Dev.
I_1	Normal	m^4	0.0021	0.0002
I_2	Normal	m^4	0.0036	0.0004
I_3	Normal	m^4	0.0067	0.0007
I_4	Normal	m^4	0.0076	0.0008
I_5	Normal	m^4	0.0038	0.0004
I_6	Normal	m^4	4.99E-3	4.99E-4
I_7	Normal	m^4	4.68E-03	4.68E-04
I_8	Normal	m^4	8.24E-03	8.24E-04

Table 2: Description of the input uncertainties and their statistical properties for the plane truss

Parameter	Distribution	Unit	Mean	Std. Dev.
E	Log-Normal	N/m^2	2.1E11	2.1E10
ρ	Weibull	kg/m^3	7850	785
A_1	Log-Normal	m^2	2E-3	2E-4
A_2	Log-Normal	m^2	1E-3	1E-4
L_1	Normal	m	1	0.05
L_2	Normal	m	0.8	0.04

Table 3: Remaining DOFs for each reduction strategy in the shear frame

Strategy	Remaining DOFs
1	1, 3, 9, and 16
2	1, 3, 6, 8, 11, and 14
3	1, 3, 5, 7, 9, 11, 13, 15, and 16

[DOI: 10.22068/ijoce.2026.16.2.679]

Table 4: Remaining DOFs for each reduction strategy in the plane truss

Strategy	Remaining DOFs (vertical direction)	Remaining DOFs (horizontal direction)
1	Nodes 1, 3, 5, 9, 12, and 14	-
2	Nodes 1, 2, 3, 4, 5, 6, 7, 9, 10, and 13	-
3	Nodes 1, 2, 3, 4, 5, 6, 7, 9, 10, 11, 12, 13, and 14	Nodes 9 and 14

4. RESULTS

The results are organised into three parts to examine the relationship between ROM accuracy and the reliability of uncertainty-based analyses. First, the predictive accuracy of the ROMs is assessed by comparing the natural frequencies predicted by different condensation techniques and master DOF selection strategies. The analysis then focuses on the capability of the ROMs to capture uncertainty propagation through comparisons of their confidence intervals with those of the FOM. Finally, GSA is conducted using the optimal reduction strategy identified for each structural model to determine how effectively the sensitivity patterns of the FOM are preserved after model reduction.

4.1 Accuracy assessment of the reduced order models

The NRFD metric for the shear frame and plane truss obtained using the three master DOF selection strategies are presented in Figures 3 and 4, respectively. Across both structures, progressively refining the retained DOFs consistently reduces the NRFD values, confirming that an appropriate master DOF configuration is essential for preserving the dynamic characteristics of the FOM. A further observation is that the extent of this improvement depends on the dynamic complexity of the structure, with the influence of master DOF selection becoming increasingly pronounced as the structural response spans a broader frequency range.

Clear differences between the investigated reduction techniques emerge as the vibration mode increases. SEREP maintains the lowest NRFD values across all reduction strategies and throughout the considered modal range, demonstrating a high degree of robustness with respect to both structural dynamic behaviour and master DOF selection. IRS also provides a close approximation to the FOM, with only limited differences appearing in the highest modes of the shear frame and slightly larger discrepancies in the plane truss under the first master DOF configuration. The Guyan and dynamic condensation methods, however, exhibit an increasingly larger separation from the FOM as the vibration mode increases. Despite the close agreement among the four techniques in the lower modes, their performance begins to differ in the higher modes, where the increasing complexity of the modal response imposes greater challenges for accurate representation.

The stronger distinction between the reduction techniques for the plane truss reflects the greater influence of structural dynamic complexity on ROM performance. Deterministic model fidelity therefore becomes more strongly dependent on the ability of a reduction

[DOI: 10.22068/ijoce.2026.16.2.679]

technique to retain higher-order dynamic characteristics, providing the foundation for the subsequent assessment of uncertainty propagation and global sensitivity.

4.2 Uncertainty propagation

Figures 5 and 6 compare the 95% confidence intervals (CIs) of the natural frequencies estimated by the FOM and the ROMs for the shear frame and plane truss, respectively. Rather than focusing on deterministic fidelity, this analysis examines how uncertainty in the input parameters is transferred to the predicted structural response after model reduction. Across both structures, the CIs widen with increasing vibration mode, indicating that higher-frequency responses are more sensitive to parameter uncertainty. This effect is substantially stronger for the plane truss, highlighting the greater role of structural dynamic complexity in governing uncertainty propagation.

The four reduction techniques exhibit distinctly different abilities to reproduce this probabilistic behaviour. SEREP consistently yields CIs that remain almost indistinguishable from those of the FOM throughout the investigated modal range and for all master DOF strategies, demonstrating that the uncertainty characteristics of the reference model are effectively retained after reduction. IRS also follows the probabilistic response closely for the shear frame, with the remaining differences becoming almost negligible under the third master DOF strategy. For the plane truss, however, noticeable discrepancies persist in the upper modal range even after refinement of the retained DOFs, indicating that the benefits of improving the master DOF configuration diminish as the structural dynamics become more complex. The Guyan and dynamic condensation methods exhibit increasingly wider CIs from the intermediate modes onwards, showing that the variability introduced by uncertain parameters is no longer fully reproduced after model reduction.

A clear correspondence exists between deterministic accuracy and the predicted CIs across the investigated reduction techniques. Reduction techniques that more accurately reproduce the modal characteristics of the FOM also retain the associated uncertainty with greater consistency. The same trend is observed for master DOF selection, where improved retained DOFs systematically reduce the differences in the predicted uncertainty bounds, with a markedly stronger effect for the shear frame than for the plane truss. This behaviour indicates that uncertainty propagation is governed not only by the reduction technique itself but also by the quality of the retained DOF configuration.

4.3 Global sensitivity analysis

Figures 7 and 8 compare the first-order and total Sobol' indices of the FOM and the ROMs for the shear frame and plane truss using the third master DOF selection strategy. Previous analyses focused on the accuracy of the predicted responses and their uncertainty ranges, while this section evaluates whether the reduction process maintains the relative importance of uncertain parameters in response variability. This aspect is critical because similarity in the predicted natural frequencies alone does not ensure that the dominant uncertainty sources and their relative contributions to response variability are accurately identified.

[DOI: 10.22068/ijoce.2026.16.2.679]

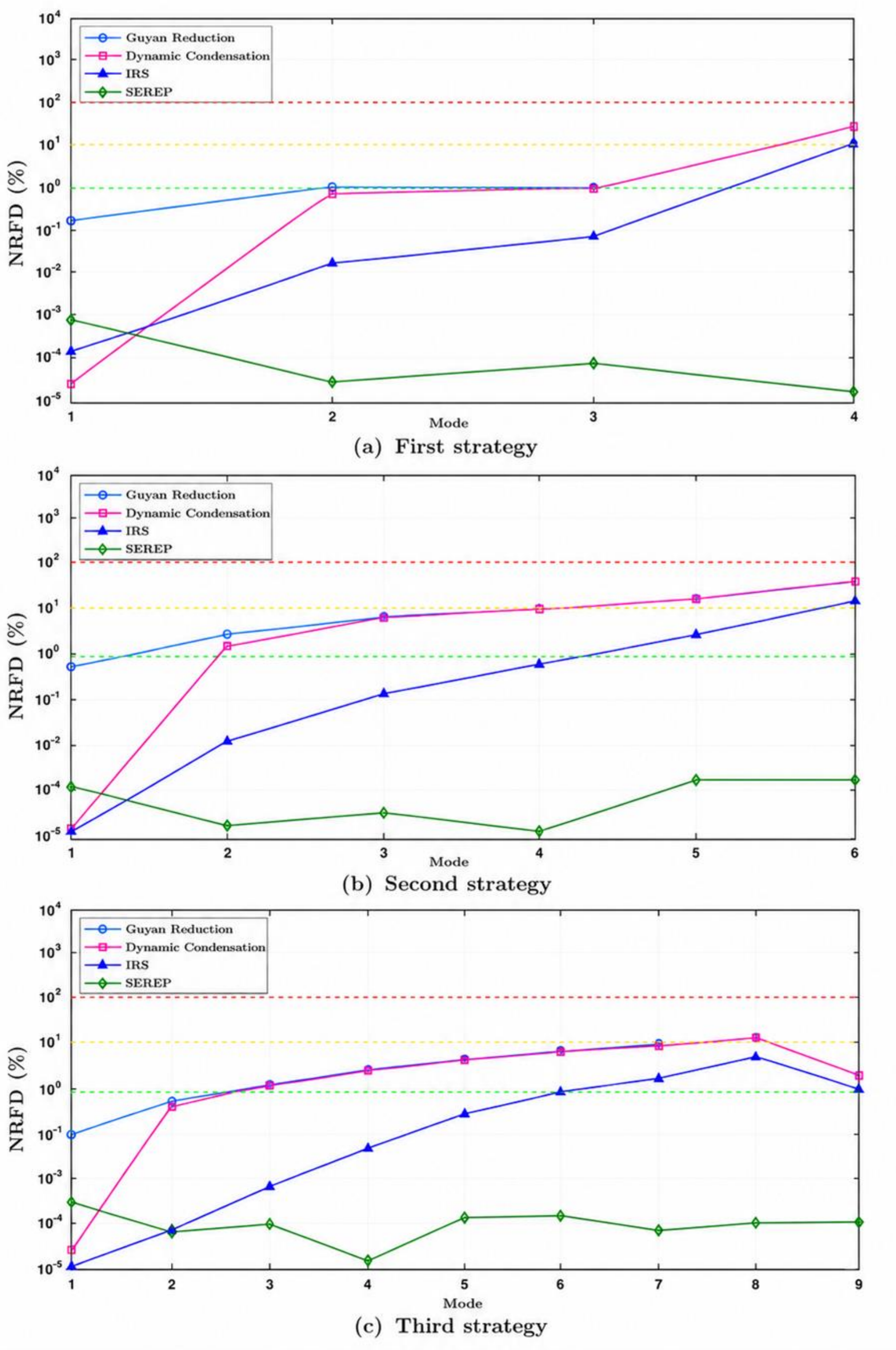

Figure 3: NRFD values for the reduced models of the shear frame

[DOI: 10.22068/ijoce.2026.16.2.679]

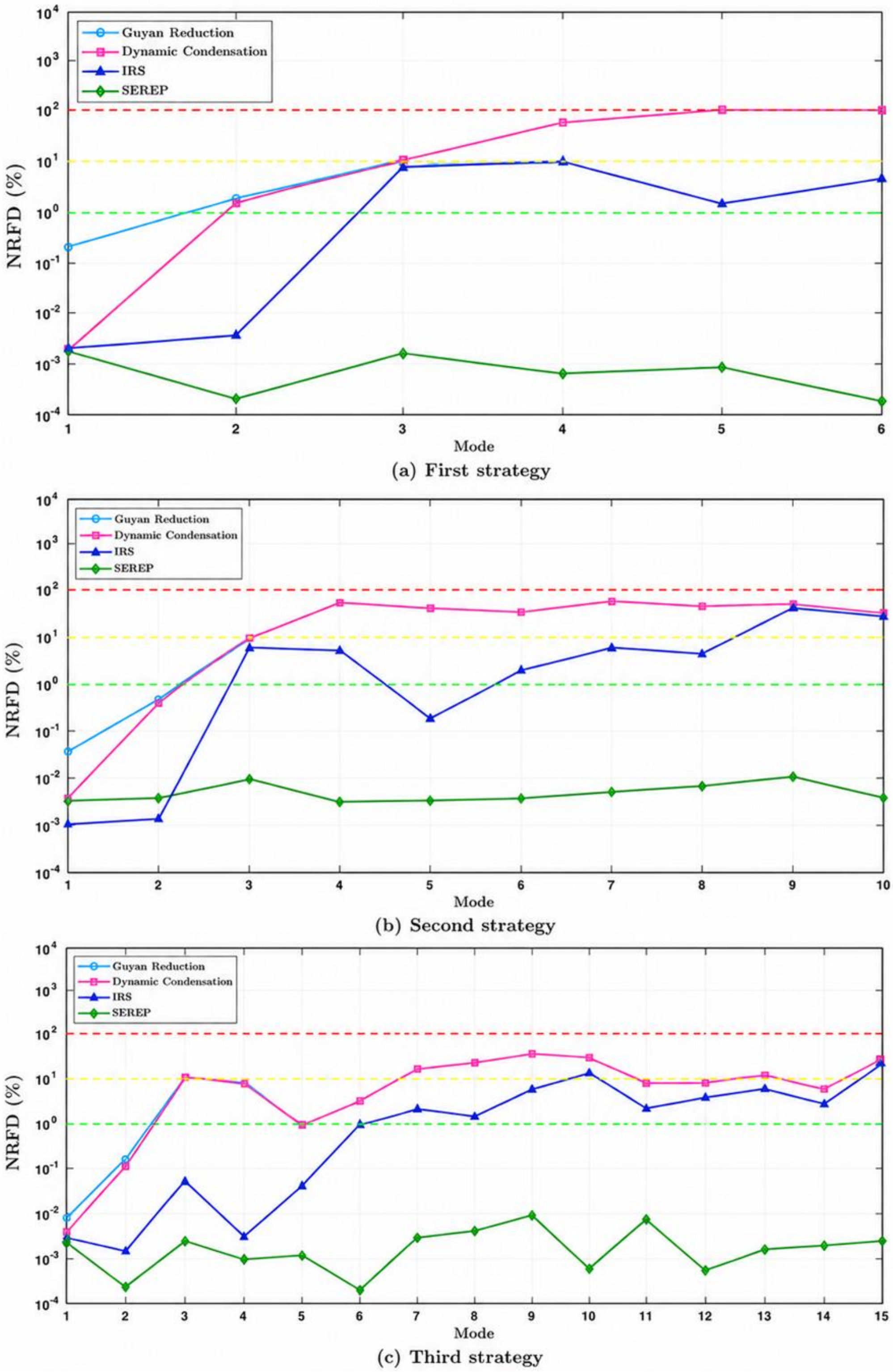

Figure 4: NRFD values for the reduced models of the plane truss

[DOI: 10.22068/ijoce.2026.16.2.679]

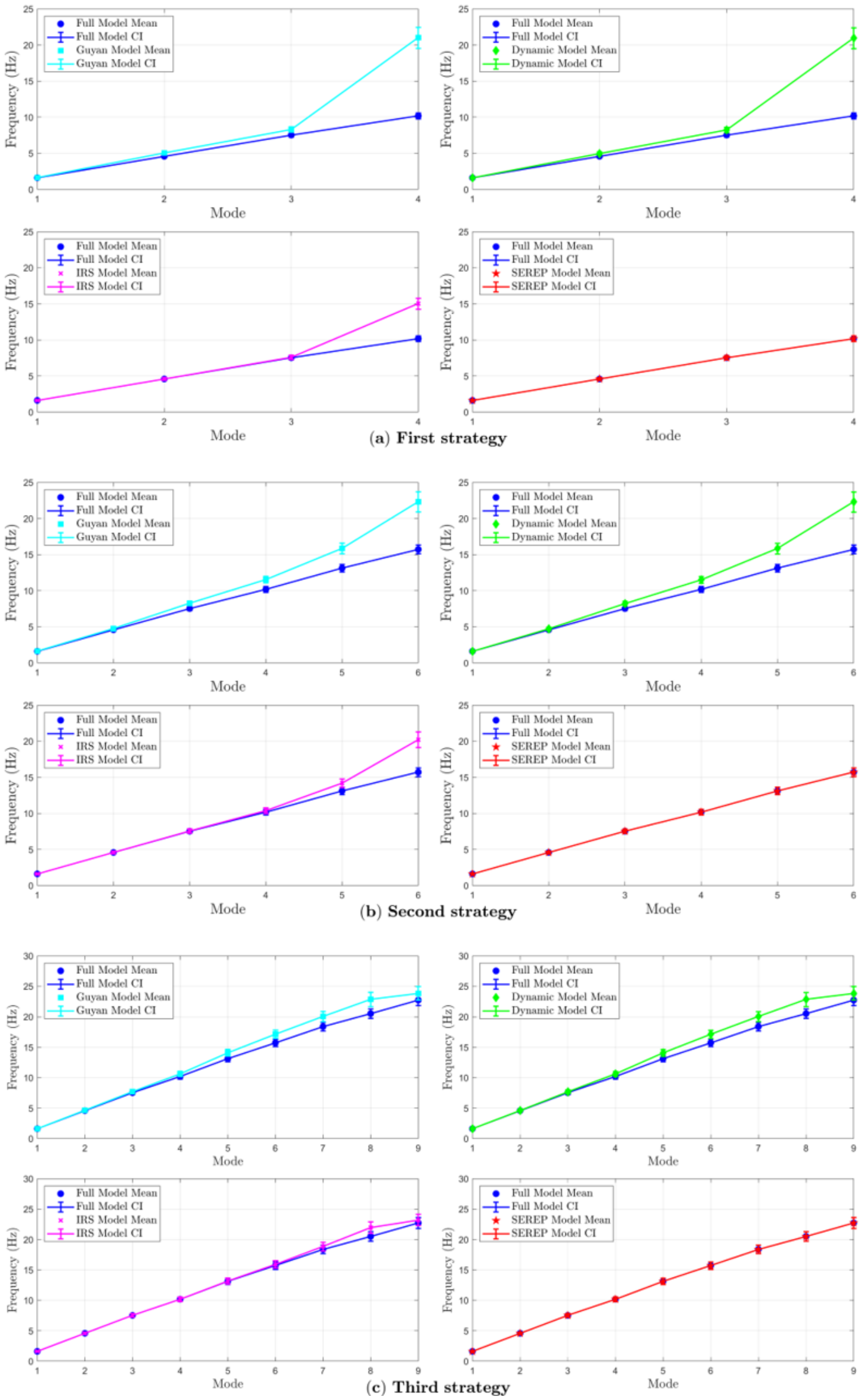

Figure 5: 95% CIs for the natural frequencies of the shear frame

[DOI: 10.22068/ijoce.2026.16.2.679]

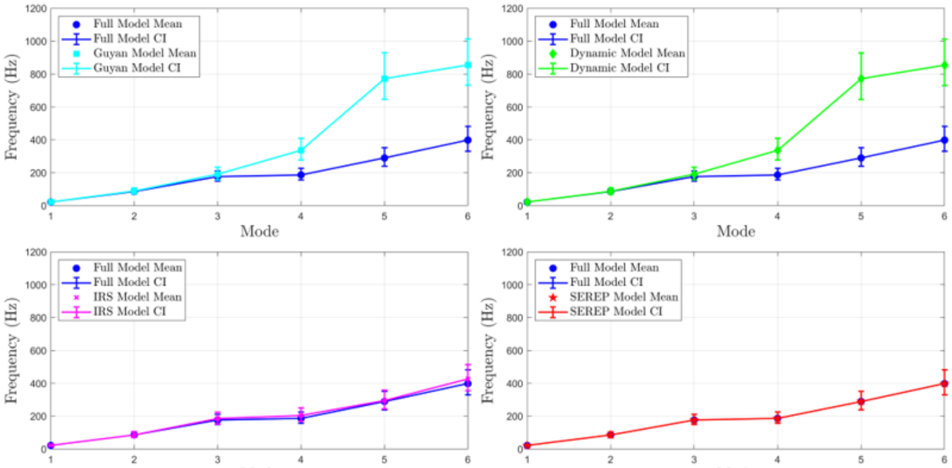

(a) **First strategy**

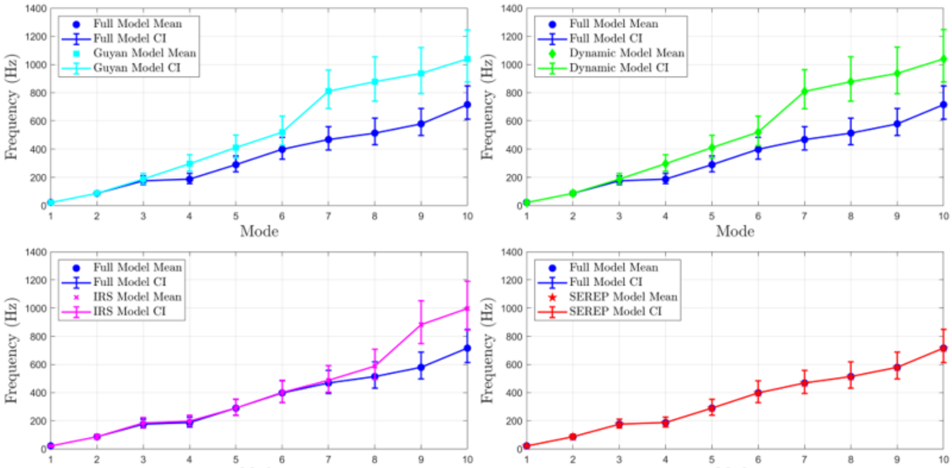

(b) **Second strategy**

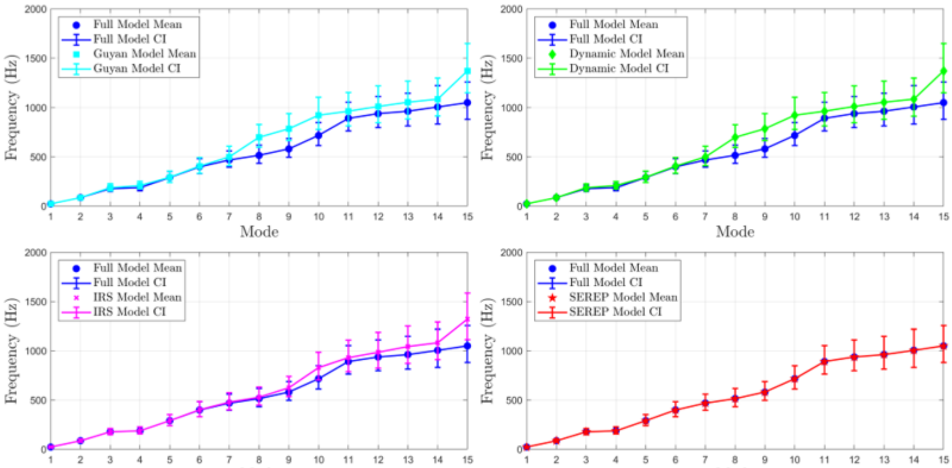

(c) **Third strategy**

Figure 6: 95% CIs for the natural frequencies of the plane truss

[DOI: 10.22068/ijoce.2026.16.2.679]

For the shear frame, the contribution of uncertain parameters varies systematically across the vibration modes. The first mode is dominated by I_5 and I_7, whereas I_2 and I_6 become the principal contributors in the second mode. In the third and fourth modes, I_3 becomes increasingly influential, while I_5 and I_7 continue to represent the major sources of variability. All reduction techniques capture the same sequence of influential parameters identified by the FOM, indicating that the interpretation of the uncertainty sources remains unchanged after reduction. The main differences between the ROMs are therefore related to the magnitude of the calculated Sobol' indices rather than to the parameters identified as the primary contributors to the response variability. SEREP provides the closest agreement with the FOM throughout the analysed modal range, followed by IRS, which exhibits only minor deviations in the higher modes. The Guyan and dynamic condensation methods show larger discrepancies in these modes; however, their deviations do not modify the ranking of the parameters with the largest impact on the response variability.

The plane truss exhibits a more complex sensitivity pattern across the vibration modes. In the first two modes, L_1 accounts for the largest share of the response variance, followed by ρ and E. In the third mode, the relative importance of these parameters changes, with ρ becoming the primary source of variability, whereas L_1 becomes the leading parameter again in the fourth mode. SEREP captures this modal transition with close agreement to the FOM, while IRS follows the same pattern with moderate differences in the estimated Sobol' indices. The Guyan and dynamic condensation methods show increasing discrepancies in the higher-order modes. Although both techniques show acceptable agreement in the lower modes, they fail to preserve the parameter ranking identified by the FOM, resulting in differences in both the sensitivity magnitudes and the ordering of the most influential variables.

Across both structural models, the first-order and total Sobol' indices remain nearly identical for all vibration modes and reduction techniques, confirming negligible interaction effects among the uncertain variables and that the response variance is largely attributed to the individual parameters. The comparison further shows that preserving the underlying sensitivity structure becomes increasingly challenging with increasing structural dynamic complexity. All reduction techniques retain the general sensitivity pattern of the shear frame, whereas the more demanding response behaviour of the plane truss exposes the limitations of simpler reduction approaches, particularly the Guyan and dynamic techniques, in preserving the FOM sensitivity structure.

5. CONCLUSIONS

This study presented a comprehensive framework for evaluating the reliability of ROMs for structural dynamic analyses under uncertainty by integrating deterministic validation, uncertainty propagation, and GSA. The results demonstrate that deterministic accuracy, although essential, is not by itself a sufficient criterion for selecting ROMs for stochastic structural dynamic analyses. The findings further show that reliable UQ depends on the ability of reduced models to preserve not only the dynamic response of the FOM but also the associated uncertainty characteristics arising from uncertain input parameters.

[DOI: 10.22068/ijoce.2026.16.2.679]

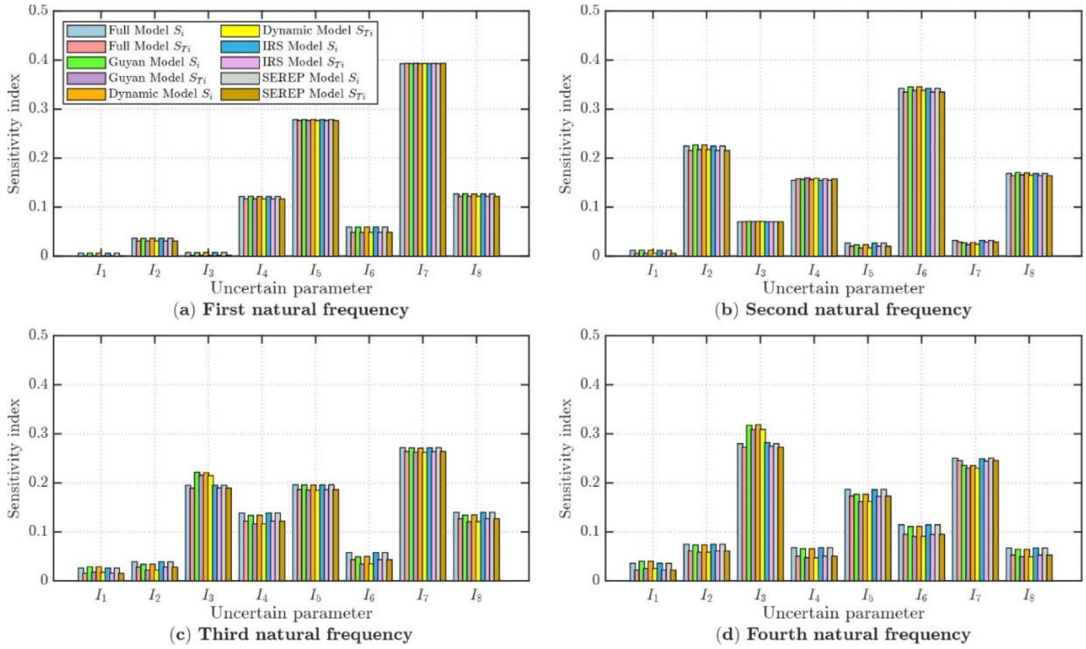

Figure 7: Sobol' indices for the first four natural frequencies of the shear frame

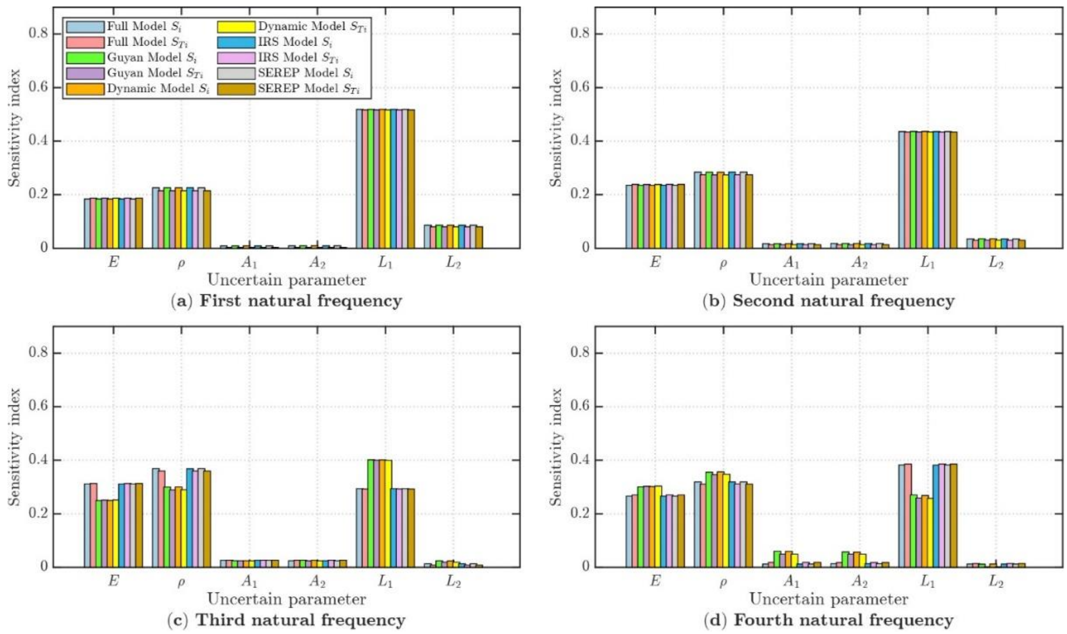

Figure 8: Sobol' indices for the first four natural frequencies of the plane truss

Comparative analyses conducted on two structural systems with distinct dynamic characteristics showed that the performance of ROMs is governed by both the selected master DOFs and the complexity of the structural response. SEREP consistently achieved the closest agreement with the FOM across all investigated vibration modes. IRS also showed strong overall performance, particularly for the shear frame, whereas moderate deviations were observed in the higher vibration modes of the plane truss. The Guyan and Dynamic condensation methods yielded satisfactory results for the lower modes, but their effectiveness gradually diminished as the contribution of higher-frequency dynamics became increasingly significant.

An important outcome of this work is the strong relationship between deterministic model fidelity and the reliability of uncertainty predictions. The reduction techniques exhibiting the highest overall accuracy also provided the closest confidence interval predictions and Sobol sensitivity estimates, correctly identifying both the dominant uncertain parameters and their relative contributions to response variability. As the approximation of the FOM became less accurate, larger discrepancies appeared in uncertainty propagation, accompanied by changes in both the ranking and the relative importance of the most influential uncertain parameters.

[DOI: 10.22068/ijoce.2026.16.2.679]

REFERENCES

1. Cao MS, Sha GG, Gao YF, Ostachowicz W. Structural damage identification using damping: a compendium of uses and features. *Smart Mater Struct*. 2017;**26**(4):043001.
2. Kaveh A, Zolghadr A. Optimal design of cyclically symmetric trusses with frequency constraints using cyclical parthenogenesis algorithm. *Adv Struct Eng*. 2018;**21**(5):739–55.
3. Hosseini P, Kaveh A, Hatami N, Hoseini Vaez SR. The optimization of large-scale dome trusses on the basis of the probability of failure. *Int J Optim Civ Eng*. 2022;**12**(3):457–75.
4. Koutsovasilis P, Beitelschmidt M. Comparison of model reduction techniques for large mechanical systems. *Multibody Syst Dyn*. 2008;**20**(2):111–28.
5. Kaveh A, Rahami H, Asl MA, Mirghaderi SR. Analysis of regular structures with member irregularity using the equilibrium equations and the singular value decomposition. *Adv Struct Eng*. 2013;**16**(5):823–44.
6. Patalano S, Mango Furnari A, Vitolo F, Dion JL, Plateaux R, Renaud F. A critical exposition of model order reduction techniques: application to a slewing flexible beam. *Arch Comput Methods Eng*. 2019;**28**(1):31–52.
7. Flodén O, Persson K, Sandberg G. Reduction methods for the dynamic analysis of substructure models of lightweight building structures. *Comput Struct*. 2014;**138**:49–61.
8. Ghannadi P, Kourehli SS. Investigation of the accuracy of different finite element model reduction techniques. *Struct Monit Maint*. 2018;**5**(3):417–28.
9. Kaveh A, Dadras A, Geran Malek N. Robust design optimization of laminated plates under uncertain bounded buckling loads. *Struct Multidiscip Optim*. 2019;**59**(3):877–91.
10. Cao R, Sun Z, Wang J, Guo F. An efficient reliability analysis strategy for low failure probability problems. *Struct Eng Mech*. 2021;**78**(2):209–18.
11. Wang Q, Wu D, Li G, Liu Z, Tong J, Chen X, Gao W. Machine learning aided uncertainty quantification for engineering structures involving material-geometric randomness and data imperfection. *Comput Methods Appl Mech Eng*. 2024;**423**(5):116868.
12. Ewing ME, Liechty BC, Black DL. A general methodology for uncertainty quantification in engineering analyses using a credible probability box. *J Verif Valid Uncert Quantif*. 2018;**3**(2):021003.

13. Zhang J, Ju Y, Wang R. Basic framework and main methods of uncertainty quantification. *Math Probl Eng*. 2020;**2020**(1):1–18.
14. Zhang J. Modern Monte Carlo methods for efficient uncertainty quantification and propagation: a survey. *WIREs Comput Stat*. 2021;**13**(5):1539.
15. Azarhoosh Z, Ilchi Ghazaan M. A review of recent advances in surrogate models for uncertainty quantification of high-dimensional engineering applications. *Comput Methods Appl Mech Eng*. 2025;**433**:117508.
16. Song C, Kawai R. Monte Carlo and variance reduction methods for structural reliability analysis: a comprehensive review. *Probab Eng Mech*. 2023;**73**:103479.
17. Kumar D, Yao K, Rauchs G, Marchi M, Kavka C, Belouettar S. Efficient uncertainty quantification and management in the early stage design of composite applications. *Compos Struct*. 2020;**251**:112538.
18. Rubinstein RY, Kroese DP. *Simulation and the Monte Carlo Method*. 3rd ed. Wiley; 2017.
19. Sudret B, Marelli S, Wiart J. Surrogate models for uncertainty quantification: an overview. *Proc 11th Eur Conf Antennas Propag (EUCAP)*. 2017.
20. Roy A, Chakraborty S. Support vector regression based metamodel by sequential adaptive sampling for reliability analysis of structures. *Reliab Eng Syst Saf*. 2020;**200**:106948.
21. Su L, Wan HP, Li Y, Ling XZ. Soil-pile-quay wall system with liquefaction-induced lateral spreading: experimental investigation, numerical simulation, and global sensitivity analysis. *J Geotech Geoenviron Eng*. 2018;**144**(11):04018087.
22. Ni P, Xia Y, Li J, Hao H. Using polynomial chaos expansion for uncertainty and sensitivity analysis of bridge structures. *Mech Syst Signal Process*. 2019;**119**:293–311.
23. Hariri-Ardebili MA, Sudret B. Polynomial chaos expansion for uncertainty quantification of dam engineering problems. *Eng Struct*. 2020;**203**:109631.
24. Maleki AT, Parviz H, Khatibi AA, Zakeri M. Probabilistic stability of uncertain composite plates and stochastic irregularity in their buckling mode shapes: a semi-analytical non-intrusive approach. *Front Struct Civ Eng*. 2023;**17**(6):179–90.
25. Wan H, Ren W, Todd MD. Arbitrary polynomial chaos expansion method for uncertainty quantification and global sensitivity analysis in structural dynamics. *Mech Syst Signal Process*. 2020;**142**:106732.
26. Wei X, Wan HP, Russell J, Živanović S, He X. Influence of mechanical uncertainties on dynamic responses of a full-scale all-FRP footbridge. *Compos Struct*. 2019;**223**:110964.
27. Ilchi Ghazaan M, Khademi A. Sensitivity analysis of compressive strength in CNT-reinforced composites: a comparative study of sample-based, linearization, and global methods. *Arab J Sci Eng*. 2024;**50**(16):12959–75.
28. Zhang H, Song Y, Zhu X, Zhang Y, Wang H, Gao Y. A surrogate model for uncertainty quantification and global sensitivity analysis of nonlinear large-scale dome structures. *Front Struct Civ Eng*. 2023;**17**(11):1813–29.
29. Liu W, Wu X, Zhang L, Wang Y, Teng J. Sensitivity analysis of structural health risk in operational tunnels. *Autom Constr*. 2018;**94**:135–53.
30. Fatehi MR, Ghanbarzadeh A, Moradi S, Hajnayeb A. Global sensitivity analysis improvement of rotor-bearing system based on the genetic based Latine hypercube sampling (GBLHS) method. *Struct Eng Mech*. 2018;**68**(5):549–61.

[DOI: 10.22068/ijoce.2026.16.2.679]

31. Etedali S. Probabilistic study on buildings with MTMD system in different seismic performance levels. *Struct Eng Mech*. 2022;**81**(4):429–41.
32. Friswell MI, Garvey SD, Penny JET. Using iterated IRS model reduction techniques to calculate eigensolutions. *Proc SPIE Int Soc Opt Eng*. 1997;**3089**:1537–43 → 1537–43 (no shortening needed).
33. Qu ZQ, Fu ZF. An iterative method for dynamic condensation of structural matrices. *Mech Syst Signal Process*. 2000;**14**(4):667–78.
34. Bouhaddi N, Fillod R. Model reduction by a simplified variant of dynamic condensation. *J Sound Vib*. 1996;**191**(2):233–50.
35. Qu ZQ. Dynamic condensation. In: *Model Order Reduction Techniques with Applications in Finite Element Analysis*. Springer; 2013:71–109.
36. Friswell MI, Garvey SD, Penny JET. The convergence of the iterated IRS method. *J Sound Vib*. 1998;**211**(1):123–32.
37. Papadopoulos M, Garcia E. Improvement in model reduction schemes using the system equivalent reduction expansion process. *AIAA J*. 1996;**34**(10):2217–19.
38. Persson P, Flodén O, Danielsson H, Peplow A, Andersen LV. Improved low-frequency performance of cross-laminated timber floor panels by informed material selection. *Appl Acoust*. 2021;**179**:108017.
39. Xiong Z, Jia G. Data-driven global sensitivity analysis for group of random variables through knowledge-enhanced machine learning with normalizing flows. *Reliab Eng Syst Saf*. 2025;**260**:111007.
40. Alves Borges LF, Freitas Ferreira F, Gonçalves F, Espósito Junior A, Da Silva Oliveira AF, Rambaldi Telles W. IPSAL: implementation of the module to generate the Sobol sequence and indices. *Vetor Rev Cienc Exatas Eng*. 2023;**33**(2):60–69.
41. Harenberg D, Marelli S, Sudret B, Winschel V. Uncertainty quantification and global sensitivity analysis for economic models. *Quant Econ*. 2019;**10**(1):1–41.
42. Chen L, Xu Z, Huang D, Chen Z. An improved Sobol sensitivity analysis method. *J Phys Conf Ser*. 2024;**2747**(1):012025.
43. Tosin M, Côrtes A, Cunha A Jr. A tutorial on Sobol' global sensitivity analysis applied to biological models. In: *Networks in Systems Biology: Applications for Disease Modeling*. Springer; 2020.
44. Goswami S, Ghosh S, Chakraborty S. Reliability analysis of structures by iterative improved response surface method. *Struct Saf*. 2016;**60**:56–66.
45. Basaga HB, Bayraktar A, Kaymaz I. An improved response surface method for reliability analysis of structures. *Struct Eng Mech*. 2012;**42**(2):175–89.
46. Zhao W, Qiu Z. An efficient response surface method and its application to structural reliability and reliability-based optimization. *Finite Elem Anal Des*. 2013;**67**:34–42.

[DOI: 10.22068/ijoce.2026.16.2.679]